Extracting the information of scattering potential using angular distributions of rescattered photoelectrons

Yan Wu,[1,2] Huiliang Ye,[1,2] and Jingtao Zhang[1,*]

[1]*State Key Laboratory of High Field Laser Physics, Shanghai Institute of Optics and Fine Mechanics, Chinese Academy of Sciences, Shanghai 201800, China*

[2]*Graduate University of Chinese Academy of Sciences, Beijing 100049, China*

(Received 16 August 2011; published 18 October 2011)

Rescattered photoelectrons are greatly affected by the binding potential of the parent core, while directly emitted photoelectrons not. They are of comparable probability amplitudes at the onset of the plateau in the kinetic energy spectra of photoelectrons, which leads to the photoelectron angular distributions varying distinctively with binding potential of the targets. We exhibit such variations and propose that the variations can be used to extract potential information of the target core.

DOI: 10.1103/PhysRevA.84.043418 PACS number(s): 32.80.Rm, 42.65.Ky, 12.20.Ds, 03.65.Nk

I. INTRODUCTION

High-order above-threshold ionization (ATI) is characterized by a broad plateau followed by a cutoff at about $10U_p$ in the photoelectron energy spectrum (PES) [1–3], where U_p is the ponderomotive energy. Generally, the generation of those high-energy photoelectrons is accounted for by the so-called rescattering mechanism [4]: When irradiated by an intense laser field, the bound electrons of atoms or molecules are excited into continuum states. Intuitively, when the electric field of the incident laser reverses, some electrons in the continuum states may be pulled back to the vicinity of their parent cores. Then the attraction of their parent cores becomes the dominant factor that governs the subsequent motion of those driven-back electrons. Some of those electrons are rescattered then escape from the laser field. The photoelectrons arising from the rescattering process have much higher kinetic energy—up to about $10U_p$—since they are further accelerated by the electric field. More importantly, the rescattered photoelectrons carry information about the potential of their parent core, thus providing a supplementary means to learn about the core structure of the target atoms and molecules [5–7].

Many efforts have contributed to this end. The ring structure in the photoelectron angular distribution (PAD) of the ATI orders at the onset of the plateau was attributed to the rescattering effect [2,8]. Milošević *et al*. showed the variation of the plateau with the screening parameter of the Yukawa potential and pointed out that the PES may be used to detect the binding potential of the target atoms [9]. Recently, Morishita *et al*. proposed that the momentum spectra of high-order ATI can be used to retrieve the core structure of the target atoms and molecules [10,11].

In our recent analytical study based on the quantum scattering theory of ATI developed by Guo, Åberg, and Creasmann [12], we reproduce the plateau structure of the PES and confirm that the high-order ATI is caused mainly by the rescattering effect of the parent core. We find that the ionization amplitude includes two parts: one is formed by the directly emitted photoelectrons in which the influence of the parent core is included only in the initial wave function, whereas the other is formed by the rescattered photoelectrons and depends explicitly on the binding potential of the parent core. The emission rate from the direct ionization decreases rapidly as the ATI order increases, whereas that from the rescattering process changes gently up to a sharp cutoff at about $10U_p$. At the onset of the plateau, the photoelectrons coming from two sources have comparable probability amplitudes, thus their interference effect is strong. Consequently, any variation of the rescattered photoelectrons becomes evident. This finding reveals the possibility to extract information about the core potential by using the rescattered photoelectrons, especially by using the photoelectrons at the onset of the plateau structure. Such a scheme has unique advantages which were not disclosed by other related studies.

In this paper, we demonstrate that the PES and the PAD at the onset of the plateau are very sensitive to the binding potential of the parent core and thus can be used to extract information on the scattering potential. The angular distributions of photoelectrons in the rest part of the spectrum do not share that property, although their absolute values also depend on the binding potential of the parent core. In order to exhibit the variation of the PES and PAD, we take two widely used model potentials as examples; namely, the Yukawa potential and the Gaussian potential. We believe that the phenomena demonstrated here can be easily expanded into other model potentials, which provides an important reference for extracting information on the scattering potential from the rescattered photoelectrons.

II. THEOETEICAL ANALYSIS

In our analytical study, we use standard perturbation theory to derive an expression for the ionzation rate of rescattered photoelectrons. Using the quantized-field Volkov states as the intermediate states [12], we obtain the differential ionization rate for a given ATI order as (the units $\hbar = c = 1$ are used)

$$\frac{dW}{d\Omega_{p_f}} = \frac{\left(2m_e^3\omega^5\right)^{1/2}}{(2\pi)^2}(q - e_b)^{1/2}|T_d + T_r|^2, \qquad (1)$$

where $d\Omega_{p_f} = \sin\theta d\theta d\phi$ is the solid angle in momentum space, in which θ is the scattering angle and ϕ is the azimuth

*jtzhang@siom.ac.cn

angle; m_e is the rest mass of the electron and q is the number of photons absorbed during the overall ionization process and denotes the ATI order. The kinetic energy of photoelectrons satisfies

$$E_k \equiv \frac{\mathbf{P}_f^2}{2m_e} = q\omega - e_b\omega, \tag{2}$$

where $\mathbf{P}_f$ is the final photoelectron momentum and $e_b\omega$ is the binding energy of the target atom. The first transition matrix element in Eq. (1) is for the directly emitted photoelectrons [12]:

$$T_d = (u_p - j_i)\mathcal{X}_{-j_i}(\zeta_f,\eta)^*\mathcal{X}_{-j_f}(\zeta_f,\eta)\Phi_i(|\mathbf{P}_f - q\mathbf{k}|), \tag{3}$$

in which $u_p = U_p/\omega$ is the ponderomotive parameter, and j_i and j_f are the numbers of absorbed photons in the excitation and the exit processes, respectively. The quantity $\Phi_i(|\mathbf{P}|)$ is the Fourier transform of the wave function of the initial bound electron, which depends on the binding potential of the target core. The second transition matrix element in Eq. (1) can be described by

$$T_r \propto -i\pi \sum_{\mathcal{E}_{\mathbf{P},n}=\mathcal{E}_f} \sum_{\mathcal{E}_{\mathbf{P}',n'}=\mathcal{E}_{\mathbf{P},n}} \langle\phi_f,n_f|\Psi_{\mathbf{P},n}\rangle \times \langle\Psi_{\mathbf{P},n}|U|\Psi_{\mathbf{P}',n'}\rangle\langle\Psi_{\mathbf{P}',n'}|V|\Phi_i,n_i\rangle, \tag{4}$$

where V is the interaction operator between the electron and the laser field and U denotes the attraction of the ionic core to the electron. The quantity $\mathcal{E}_{\mathbf{P},n}$ is the eigenenergy of the quantized-field Volkov state $|\Psi_{\mathbf{P},n}\rangle$, in which $\mathbf{P}$ is the momentum of the electron and n is the number of background photons [12]. The summations are performed over all the Volkov states with the same eigenenergy. The first factor of Eq. (4), from the right, describes the excitation of the initially bound electron to a Volkov state under the action of the laser field, and the third factor describes the exit process of the electron from the Volkov state to the final plane wave state, while the second factor describes the transition from a Volkov state to another on-energy-shell Volkov state under the attraction of the ionic core. Thus, the T_r term describes the rescattering amplitude of on-energy-shell transitions. It is

$$T_r = \frac{im_e}{4\pi^{3/2}}\sum_{j_i}\mathcal{X}_{-j_f}(\zeta_f,\eta)(u_p - j_i)|\mathbf{P}|\Phi_i(|\mathbf{P}|)\int d\Omega_{\mathbf{P}}X_{q-j_i+j_f} \times (\zeta - \zeta_f)\mathcal{X}_{-j_i}(\zeta,\eta)^*U(\mathbf{P}_f - \mathbf{P} - q\mathbf{k}), \tag{5}$$

where $|\mathbf{P}| = (2m_e\omega)^{1/2}(j_i - u_p - e_b)^{1/2}$ and $U(\mathbf{P})$ is the Fourier transform of the binding potential. In our calculations, we set u_p equal to j_f [12]. The (generalized) phased Bessel functions are defined as [13]

$$X_n(z) \equiv J_n(|z|)e^{in\arg(z)}, \qquad \mathcal{X}_j(z,z') \equiv \sum_{m=-\infty}^{\infty} X_{j-2m}(z)X_m(z'), \tag{6}$$

where z and z' are complex variables and the arguments in Eqs. (3) and (5) are given by

$$\zeta_f = \zeta_0\mathbf{P}_f\cdot\epsilon, \quad \zeta = \zeta_0\mathbf{P}\cdot\epsilon, \quad \eta = u_p\epsilon\cdot\epsilon/2, \tag{7}$$

where $\zeta_0 = 2\sqrt{u_p/(m_e\omega)}$ and ϵ is the polarization vector of the laser beam.

From the transition matrix elements we see that, for the directly emitted photoelectrons, the effect of the binding potential only exists in the initial wave function. Although in the ionization process the parent core may affect the photoelectrons more or less, generally the effect is weak compared with that of the intense laser field. This is the physical origin of the widely used strong-field approximation. However, for the rescattered photoelectrons, besides the initial wave function, the convolution of the binding potential $U(\mathbf{P}_f - \mathbf{P} - q\mathbf{k})$ also appears explicitly in the transition matrix, which implies that the effect of the binding potential is accumulated during the rescattering process. This effect becomes more important when the photoelectrons move in the vicinity of the parent core. As a result, the subsequent motion of the rescattered photoelectrons is implanted with information about the potential of the target atoms. Thus, using the rescattered photoelectrons to acquire information about the core attracted much attention by the end of the last century. Several observables, such as the PES and the momentum distribution, were used to extract structure information from targets [10,14]. Our study shows that the angular distribution of the photoelectrons at the onset of the PES plateau provides a convenient tool for that purpose. The advantage of using the PAD lies in the fact that the shape of the PAD indicates the relative variation of the ionization rate and PADs can be easily and exactly detected in experiments. The reason to use the PAD at the onset of the plateau is as follows: Low-energy photoelectrons, generally with kinetic energy less than $2U_p$, are mainly directly emitted and thus carry less information about the parent core. In the onset region of the plateau, generally with kinetic energy of about $2U_p$, both directly emitted and rescattered photoelectrons are of comparable probability amplitudes, so interference becomes evident. Since directly emitted photoelectrons are affected less by the core, any trivial difference in the rescattering amplitudes will greatly change the PAD, thus the PAD becomes very sensitive to the binding potential of the parent core. For photoelectrons with energy far larger than $2U_p$, however, the PAD becomes less dependent on the binding potential, since the photoelectrons come mainly from the rescattering process and the binding potential just provides a common factor related to the emission rate.

III. NUMERICAL RESULTS

In analytical calculations, the model potentials are commonly used to mimic the real potential which is determined by the inner electron distribution and cannot be described simply by the Coulomb potential [9]. By adjusting the parameters of the model potentials, the real potential is described more accurately. In the following, employing the Yukawa potential and the Gaussian potential, we calculate the energy spectra and angular distributions of photoelectrons to show their variation with the parameters of the model potentials. The Yukawa potential can be expressed as [15]

$$U_Y(\mathbf{r}) = -\frac{Ze^2}{4\pi r}\exp(-\lambda r), \tag{8}$$

where Z denotes the charge number of the ionic core and λ is the screening parameter, which can be changed to suit different ionic binding potentials. Once $r \geqslant 1/\lambda$, the potential goes

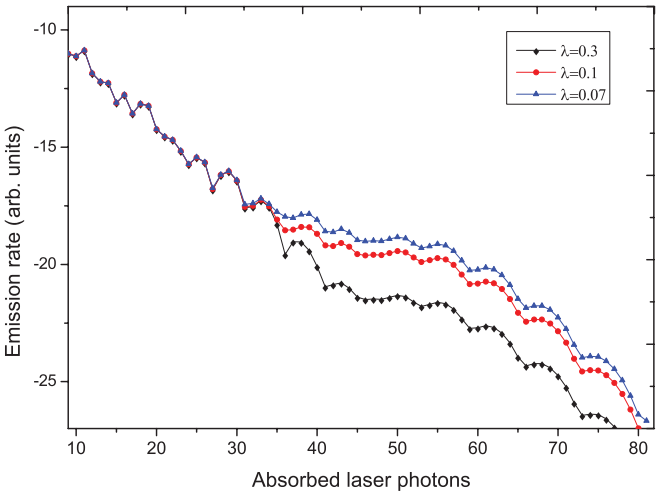

FIG. 1. (Color online) Calculated energy spectra for photoelectrons rescattered by the Yukawa potential with several screening parameters. We set $Z = 1$.

rapidly to zero; when $\lambda \to 0$, the Yukawa potential becomes the Coulomb potential, thus it is also called the screened Coulomb potential. Its Fourier transform is

$$U_Y(\mathbf{P}) = -\frac{Ze^2}{|\mathbf{P}|^2 + \lambda^2}. \tag{9}$$

The variation of this potential is performed by changing the value of λ. The Gaussian potential is given by [16]

$$U_G(r) = -U_0 \exp\left(-r^2/r_0^2\right), \tag{10}$$

where the parameter U_0 mainly determines the height of the potential well and r_0 mainly determines the gradient of the potential well. The Fourier transform is

$$U_G(\mathbf{P}) = -U_0 r_0^3 \pi^{3/2} \exp\left(-|\mathbf{P}|^2 r_0^2/4\right). \tag{11}$$

The variation of this potential is performed by changing the value of r_0. In the following we will show the variation of PADs with those parameters. The wave function is chosen to be that of a hydrogen-like $1s$ state. The driving laser field is linearly polarized at 800 nm with an intensity of 1.5×10^{14} W/cm^2. In our calculations, we set the scattering angle $\theta = \pi/2$, and the PAD is obtained by varying the azimuth angle ϕ from 0 to 2π.

The calculated PES and PAD using the Yukawa potential for several values of the screening parameter are shown in Figs. 1 and 2, respectively. From Fig. 1 we see that each PES exhibits a plateau following the falloff at the low-energy region and followed by a cutoff at about $10U_p$. As the screening parameter decreases, the height and the width of the plateau increase. Physically, a smaller screening parameter implies the attraction of the parent core to the photoelectrons decreasing slowly; that is, the attraction of the parent core affects a relatively large range so that more photoelectrons are rescattered. However, the cutoff of the plateau is independent of the screening parameter since the maximal photoelectron kinetic energy is determined mainly by the laser field. Such variation in PES was also demonstrated by Milošević *et al.* using the generalized Keldysh-Faisal-Reiss theory [9].

Figure 2 depicts the variation of PAD with the screening parameter. The PADs in each row are of the same ATI order, but

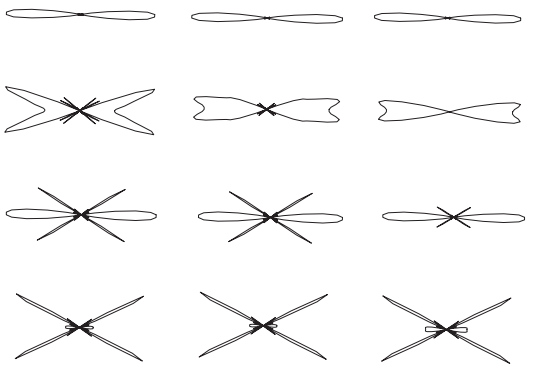

FIG. 2. Polar plots of the PADs calculated using the Yukawa potential. The PADs from the top to the bottom row are of the 28th, 35th, 42nd, and 45th ATI, respectively. The screening parameter in each column is 0.07 (left), 0.1 (middle), and 0.3 (right).

for different λ. We see that the PADs at the onset of the plateau change significantly with the screening parameter, while not for the photoelectrons in the falloff region of the PES and those in the rest of the plateau. The PADs shown in the top row are for the 28th ATI order, which is formed mainly by directly emitted photoelectrons. We see that the PADs are of the same shape, and the difference is a common factor that depends on the emission rate. The PADs shown in the bottom row are for the 45th ATI order, which is formed mainly by the rescattered photoelectrons. The PADs are of the same shape and also change less with screening parameter. Other PADs are for photoelectrons at the onset of the plateau, and their shapes vary distinctively with the screening parameter for the same ATI order. Milošević *et al.* also studied the angular distributions of rescattered photoelectrons but in the cutoff region, and they ascribed the PAD rings to the cutoff of the plateau [9].

The variation of PADs with the binding potential of the parent core is not only limited to the Yukawa model potential and does not hold only for hydrogen-like atoms. It is a general feature resulting from the physical origin of the rescattering

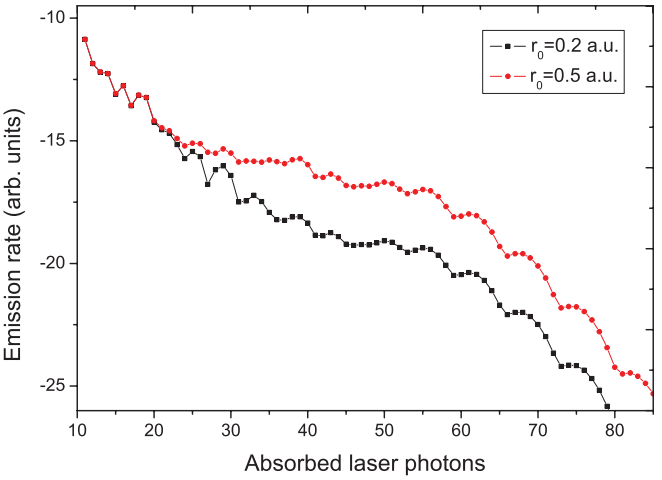

FIG. 3. (Color online) Calculated energy spectra of photoelectrons rescattered by the Gaussian potential with several r_0. We set $U_0 = 60$ eV.

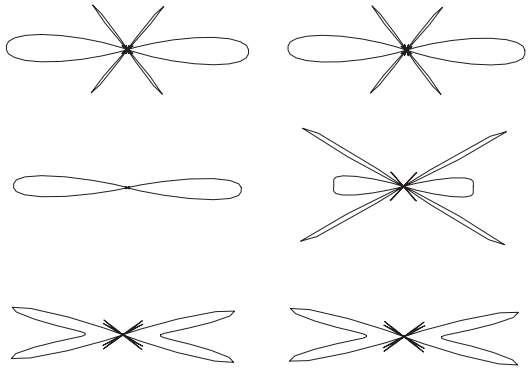

FIG. 4. Polar plots of the PADs calculated using the Gaussian potential. The PADs in the first, second, and third rows are for the 15th, 30th, and 40th ATI, respectively. The value of r_0 for the left and right columns is 0.2 and 0.5, respectively.

process. In order to show its generality, we take another widely used model potential—the Gaussian potential—to show the dependence. In Figs. 3 and 4 we depict the calculated PES and the PADs using the Gaussian potential for several values of r_0. As the parameter r_0 increases, the height and width of the plateau increase. Since r_0 mainly determines the gradient of the potential well and a smaller parameter r_0 implies a steeper potential well, a bigger r_0 means a larger range affected by the parent core, and then more photoelectrons are rescattered. Consequently, the plateau becomes higher and wider, as shown in Fig. 3. Several PADs are depicted in Fig. 4. We see that the PADs of the 15th and 40th ATI orders are almost identical for different r_0, while the PADs at the onset of the plateau (e.g., the 30th ATI) vary significantly with r_0. The results for the Gaussian potential are qualitatively the same as those for the Yukawa potential.

How does one extract the information on the scattering potential for a given atom from the experimental data of the the rescattered photoelectrons? In order to do this, one needs a reference that is obtained by theoretical calculations of the atoms with the same binding energy and the known wave function irradiated by an identical laser field. The differences between the experimental data and the model calculations originate from the different core structures. In performing the model calculations, one may use the scaling law of rescattered photoelectrons [17,18].

IV. CONCULSIONS

The photoelectrons of high-order ATI come from two sources: directly emitted photoelectrons and rescattered photoelectrons. Rescattered photoelectrons are greatly affected by the binding potential of the parent core, whereas directly emitted photoelectrons not. They are of comparable probability amplitudes at the onset of the PES plateau. This leads to the PADs at the onset of the plateau varying distinctively with the binding potential of the target atoms. In this paper, we exhibit the variations of the PADs with the binding potential and propose that such variations can be used to extract information on the scattering potential of the target core.

ACKNOWLEDGMENTS

We thank D.-S. Guo and Ruxin Li for suggestive discussions. This work was supported by the Chinese NSF under Grants No. 10774153, No. 61078080, and No. 11174304, and by the 973 Program of China under Grants No. 2010CB923203 and No. 2011CB808103.

[1] K. J. Schafer, B. Yang, L. F. DiMauro, and K. C. Kulander, Phys. Rev. Lett. **70**, 1599 (1993).
[2] B. Yang, K. J. Schafer, B. Walker, K. C. Kulander, P. Agostini, and L. F. DiMauro, Phys. Rev. Lett. **71**, 3770 (1993).
[3] G. G. Paulus, W. Nicklich, H. Xu, P. Lambropoulos, and H. Walther, Phys. Rev. Lett. **72**, 2851 (1994).
[4] G. G. Paulus, W. Becker, W. Nicklich, and H. Walther, J. Phys. B **27**, L703 (1994).
[5] M. Busuladžić, A. Gazibegović-Busuladžić, D. B. Milošević, and W. Becker, Phys. Rev. Lett. **100**, 203003 (2008); Phys. Rev. A **78**, 033412 (2008).
[6] Y. Guo, P. Fu, Z.-C. Yan, J. Gong, and B. Wang, Phys. Rev. A **80**, 063408 (2009).
[7] H. Kang *et al.*, Phys. Rev. Lett. **104**, 203001 (2010).
[8] M. Lewenstein, K. C. Kulander, K. J. Schafer, and P. H. Bucksbaum, Phys. Rev. A **51**, 1495 (1995).
[9] D. B. Milošević and F. Ehlotzky, Phys. Rev. A **57**, 5002 (1998); **58**, 3124 (1998).
[10] T. Morishita, A.-T. Le, Z. Chen, and C. D. Lin, Rev. Lett. **100**, 013903 (2008); M. Okunishi, T. Morishita, G. Prümper, K. Shimada, C. D. Lin, S. Watanabe, and K. Ueda, Phys. Rev. Lett. **100**, 143001 (2008).
[11] M. Okunishi, H. Niikura, R. R. Lucchese, T. Morishita, and K. Ueda, Phys. Rev. Lett. **106**, 063001 (2011).
[12] D.-S. Guo, T. Å. berg, and B. Crasemann, Phys. Rev. A **40**, 4997 (1989).
[13] X. Hu, H. X. Wang, and D.-S. Guo, Can. J. Phys. **86**, 863 (2008).
[14] Z. Chen, A.-T. Le, T. Morishita, and C. D. Lin, Phys. Rev. A **79**, 033409 (2009).
[15] H. Yukawa, Proc. Phys. Math. Soc. Jpn. **17**, 48 (1935).
[16] T. W. Chen, Phys. Rev. C **30**, 585 (1984); J. Gu and J.-Q. Liang, Phys. Lett. A **323**, 132 (2004).
[17] D-S. Guo, J. Zhang, Z. Xu, X. Li, P. Fu, and R. R. Freeman, Phys. Rev. A **68**, 043404 (2003).
[18] H. Ye, Y. Wu, J. Zhang, and D.-S. Guo, Opt. Exp. **19**, 20849 (2011).